

## Article

# Spatiotemporal Pattern of Vegetation Ecology Quality and Its Response to Climate Change between 2000–2017 in China

Chao Li <sup>1,2,3</sup>, Xuemei Li <sup>1,2,3,\*</sup>, Dongliang Luo <sup>4</sup>, Yi He <sup>1,2,3</sup>, Fangfang Chen <sup>4</sup>, Bo Zhang <sup>1,2,3</sup> and Qiyong Qin <sup>1,2,3</sup>

- <sup>1</sup> Faculty of Geomatics, Lanzhou Jiaotong University, Lanzhou 730070, China; 13637327312@163.com (C.L.); heyi8738@163.com (Y.H.); 18235118550@163.com (B.Z.); qinqiyong2021@163.com (Q.Q.)
- <sup>2</sup> Gansu Provincial Engineering Laboratory for National Geographic State Monitoring, Lanzhou 730070, China
- <sup>3</sup> National-Local Joint Engineering Research Center of Technologies and Applications for National Geographic State Monitoring, Lanzhou 730070, China
- <sup>4</sup> State Key Laboratory of Frozen Soil Engineering, Northwest Institute of Eco-Environmental Resources, Chinese Academy of Sciences, Lanzhou 730000, China; luodongliang@gmail.com (D.L.); 18390242783@163.com (F.C.)
- \* Correspondence: shuimingren@163.com; Tel.: +86-1779-4268-162

**Abstract:** Vegetation ecology quality (VEQ) is an important indicator for evaluating environmental quality and ecosystem balance. The VEQ in China has changed significantly with global warming and gradual intensification of human activities. It is crucial to research the spatiotemporal characteristics of VEQ and its response to climate change in China. However, most previous studies used a single indicator to reflect VEQ in China, which needs to combine the effects of multiple indicators to reveal its variation characteristics. Based on the six remote sensing indicators, fractional vegetation cover, leaf area index, net primary productivity, vegetation wetness, land surface temperature, and water use efficiency of vegetation, the vegetation ecology quality index (VEQI) was constructed by principal component analysis in this paper. The spatio-temporal distribution and trend characteristic of VEQ within disparate ecosystems in China from 2000 to 2017 were studied. How continuous climate change affected VEQ over time was also analyzed. The results showed that the differences in spatial distribution between the excellent and poor VEQ regions were significant, with the proportion of excellent regions being much larger than that of poor regions. The VEQ has been ameliorated continuously during the past 18 years. Simultaneously, the VEQ would be ameliorated persistently in the future. Differences in the distribution and variation trend of VEQ occurred in disparate ecosystems. The VEQ of broadleaved forest was the best, while that of shrubs and arctic grassland ecosystem was the worst. The VEQ characteristics were different in disparate climate zones, with the best VEQ in the tropical monsoon climate zone and the worst in the plateau mountain climate zone. Except for desert vegetation and paddy field-dominated vegetation, VEQ of other ecosystems were significantly negatively correlated with altitude. Generally, moderate precipitation and temperature were favorable to improve VEQ in China. VEQ during the peak growing season was negatively correlated with temperature and positively correlated with precipitation, and the influence of precipitation on VEQ was stronger than that of temperature. Our results can be used to enact relevant management measures and policies.

**Keywords:** vegetation ecology quality; principal component analysis; SEN + Mann–Kendall; climatic factor; China



**Citation:** Li, C.; Li, X.; Luo, D.; He, Y.; Chen, F.; Zhang, B.; Qin, Q. Spatiotemporal Pattern of Vegetation Ecology Quality and Its Response to Climate Change between 2000–2017 in China. *Sustainability* **2021**, *13*, 1419. <https://doi.org/10.3390/su13031419>

Received: 31 December 2020  
Accepted: 27 January 2021  
Published: 29 January 2021

**Publisher's Note:** MDPI stays neutral with regard to jurisdictional claims in published maps and institutional affiliations.



**Copyright:** © 2021 by the authors. Licensee MDPI, Basel, Switzerland. This article is an open access article distributed under the terms and conditions of the Creative Commons Attribution (CC BY) license (<https://creativecommons.org/licenses/by/4.0/>).

## 1. Introduction

The quality of ecological environment can reflect the suitability of ecological environment for human survival and sustainable development of the social economy. In the past twenty years, the rapid development of China's economy has led to the deterioration of the ecological environment in some regions (e.g., the southwestern Qinghai-Tibet Plateau, the western Hunshandake Sandy Area, and the northern Tianshan Mountains) [1]. To

reverse the deterioration of the ecological environment, the relevant departments took some ecological measures (e.g., the Grain for Green Program, Afforestation, wetland protection and irrigation). However, the contradictions between ecological protection and economic development are still prominent in China, and the ecological safety situation is still serious [2]. The ecological environment is composed of living and non-living organisms [3]. Eco-environmental quality assessment is used to quantify the regional quality of the ecological environment based on multiple selected indicators taking evaluation methods comprehensively [4,5]. However, the vast land area and complex terrain of China make it difficult to obtain data on species structure (e.g., uniformity and abundance of animal and microbial factors). Meanwhile, species structure data are highly uncertain and difficult to quantify. The vegetation could provide many ecological services (e.g., purifying air, conserving water, regulating climate, preventing wind, fixing sand, and landscaping) [6]. It is a monumental part of the terrestrial ecosystem, as well as a pivotal link connecting natural geographical environment elements (e.g., atmosphere, water, biology, rock and soil) [7–9]. Therefore, vegetation ecology quality (VEQ) is an extremely important indicator to reflect the environmental quality and ecosystem balance. It is necessary to quantitatively evaluate and analyze the variation trend of VEQ and its response to climate change in China over the past two decades.

With the rapid development and widespread use of remote sensing technology in recent years, the study of VEQ by remote sensing has become more common, with diverse scales, wide range, and long time series [6]. At a national scale, numerous researchers have conducted extensive studies on vegetation characteristics in China through remote sensing, including leaf area index (LAI), fractional vegetation cover (FVC), gross primary productivity (GPP), net primary productivity (NPP), evapotranspiration, water use efficiency (WUE), vegetation temperature, etc. [10,11]. LAI can reflect the growth structure and biological characteristics of vegetation [12]. FVC can represent the growth condition and cover degree of vegetation [11]. GPP and NPP can illustrate the photosynthetic intensity of plants [13]. Vegetation evapotranspiration not only affects the growth, development, and yield of plants, but also influences atmospheric circulation and plays a role in regulating climate [14]. WUE characterizes the degree of carbon and water coupling and measures the growth condition of vegetation [15]. Vegetation temperature is a good characterization of vegetation change and a pivotal factor driving variation of the ecological environment. However, the above-mentioned studies only used a single indicator to reflect VEQ. Evaluation and monitoring of a single indicator can only illustrate the change of VEQ in a certain dimension, while it needs to combine with the comprehensive impact of multiple indicators to explain the characteristics of VEQ and its variations.

Vegetation in China was taken as the evaluation object, and the main abiotic factors that characterize the growth of vegetation and affect its growth were used as indicators for evaluation. Six indicators of VEQ, including FVC, LAI, NPP, WUE, wetness (WET), and land surface temperature (LST), obtained from MODIS data and other remote sensing data from 2000 to 2017 were finally selected. Based on the principal component analysis method, the above-mentioned indicators were processed by dimensionality reduction and decorrelation. Sequentially, the vegetation ecology quality index (VEQI) was constructed. The objectives of this study are as follows: (1) to propose an assessment method of VEQ based on remote sensing data in China and reveal the spatio-temporal distribution and variation of VEQ over the past 18 years, as well as future trends; (2) to compare VEQ among different ecosystems; and (3) to analyze the relationship between VEQ and continuously changing climate factors. This study could evaluate the effectiveness of ecological restoration measures (e.g., the Afforestation and Grain for Green Program in China), and it also provides a scientific basis for the construction of ecological civilization and sustainable economic and social development in China.

## 2. Materials and Methods

### 2.1. Remote Sensing Data

Seven basic categories of remote sensing data, a total of 22 tiles (H25-26V03, H23-27V04, H23-28V05, H25-29V06, H28-29V07, H28-29V08) from 2000 to 2017, including 32,076 images for China were utilized in this study. The data of surface reflectance (MOD09A1), LST (MOD11A2), normalized vegetation index (MOD13A3), LAI (MOD15A2H), and GPP (MOD17A2H) were downloaded from the NASA data center (<https://ladsweb.modaps.eosdis.nasa.gov/search/>). The data of NPP and surface evapotranspiration (GLASS ET) were downloaded from the Ministry of Ecological Environment of the People's Republic of China (<http://www.chinageoss.cn/>) and National Earth System Science Data Center (<http://www.geodata.cn/>), respectively. The peak vegetation growth season, July–September from 2000 to 2017 was chosen as the study period for easily distinguishing between vegetated and non-vegetated regions.

To improve the accuracy of the VEQ assessment, data with low cloudiness and high quality were further screened to calculate the average value of the indicators in July–September. After mosaic, format conversion, reprojection, and resampling (1 km 1 km) by the MRT software, the Savitzky–Golay filter, exponent calculation, and mask extraction were performed using the ENVI 5.3 software.

### 2.2. Other Data

The 1-km resolution elevation data (Figure 1a) and the distribution map of vegetation types (Figure 1b) in China were chiefly downloaded from the Cold and Arid Region Scientific Data Center (<http://data.casnw.net/>). The elevation data was subjected to strict manual quality control with high accuracy [16,17]. The distribution map of vegetation types includes seven categories of natural vegetation and three categories of cultivated vegetation. The previously compiled vegetation map may not be able to fully match the latest vegetation distribution change in China due to the continuous variation of land use. In addition, the climatic zoning data in China (Figure 1c) was downloaded from the Resource and Environment Science and Data Center (<http://www.resdc.cn/>).

The data of monthly-scale precipitation and temperature with 1-km resolution from July to September during 2000–2017 were downloaded from the National Tibetan Plateau Data Center (<http://data.tpdc.ac.cn/>) (Figure 1d,e). The above data were generated at a downscaled scale in China through the spatial downscaling program of Delta based on the global 0.5° climate data published by CRU and the global high-resolution climate dataset published by WorldClim. The data were then validated by using observation data from 496 independent meteorological stations [18–22].

### 2.3. Methods

Six indicators of the VEQ were employed as evaluation indicators for the proposed VEQI, namely, vegetation greenness, thickness, productivity, moisture, heat, and growth suitability. These factors can reflect the VEQ situation and are often used to evaluate vegetation ecosystems. This study acquired information about six indicators based on remote sensing data, *FVC*, *LAI*, *NPP*, *WET*, *LST*, and *WUE*, which can represent vegetation greenness, thickness, productivity, moisture, heat, and growth suitability, respectively. Therefore, the constructed VEQI can be expressed as the following function:

$$VEQI = f(\text{Greenness, Thickness, Productivity, Moisture, Heat, Suitability}) \quad (1)$$

Remote sensing is defined as follows:

$$VEQI = f(FVC, LAI, NPP, WET, LST, WUE) \quad (2)$$

#### 2.3.1. Indicators Used in VEQI

(1) Greenness indicator (*FVC*) (Figure 2a): *FVC* can reflect the growth condition and the coverage extent of vegetation and represent the greenness indicator of vegetation. The

vegetation cover status in China has been studied by relevant scholars through remote sensing technology [11,23]. The *NDVI* data were obtained from MOD13A3 and *FVC* was calculated by pixel dichotomy, expressed as follows:

$$NDVI = NDVI_m \times FVC + NDVI_s \times (1 - FVC) \tag{3}$$

$$FVC = (NDVI - NDVI_s) / (NDVI_m - NDVI_s) \tag{4}$$

where *NDVI* and *FVC* represent the *NDVI* and *FVC* of the vegetation region, respectively. *NDVI<sub>m</sub>* and *NDVI<sub>s</sub>* characterize the maximum and minimum values of *NDVI*, which correspond to 99.5% and 0.5% of the *NDVI* values in the image frequency accumulation table, respectively.

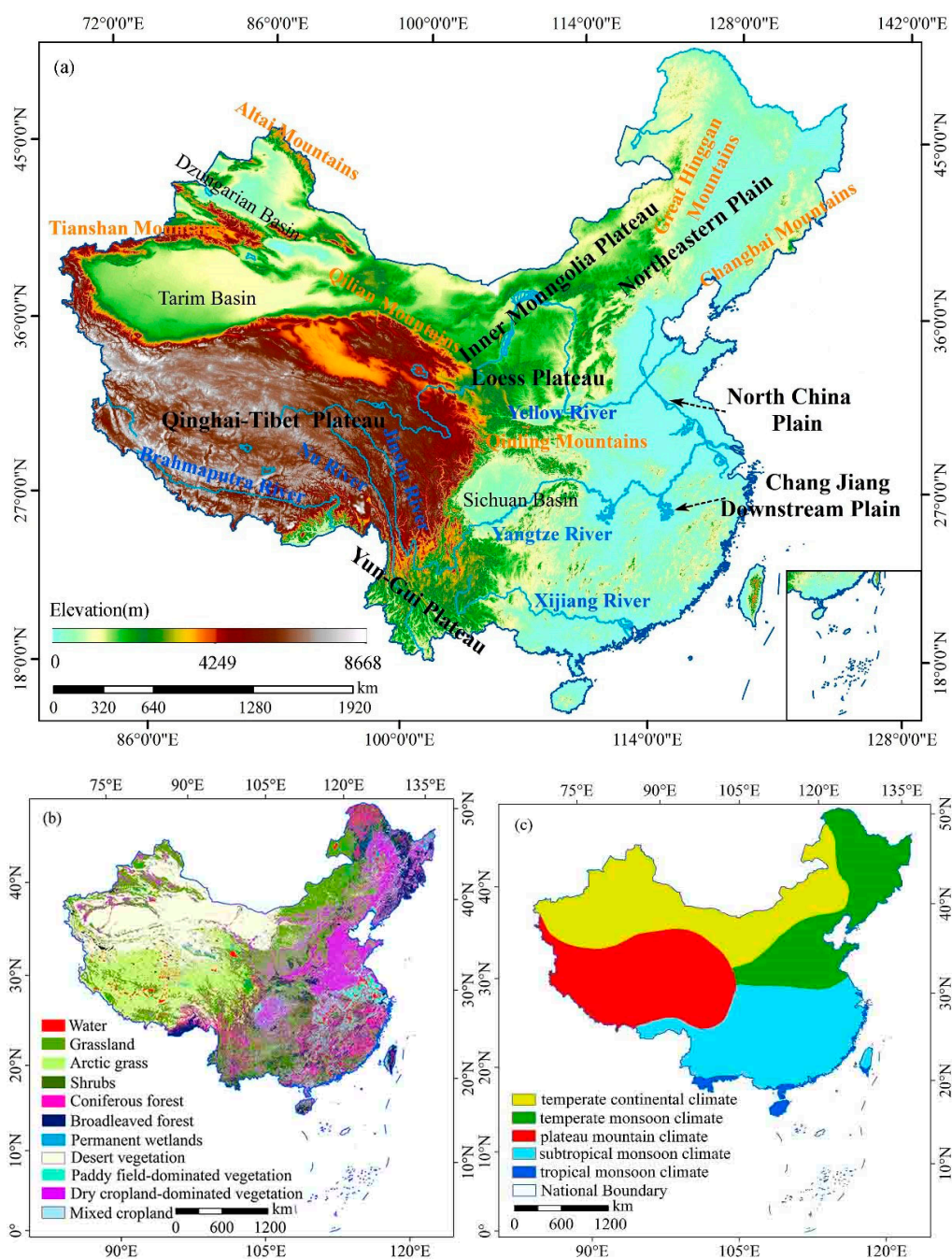
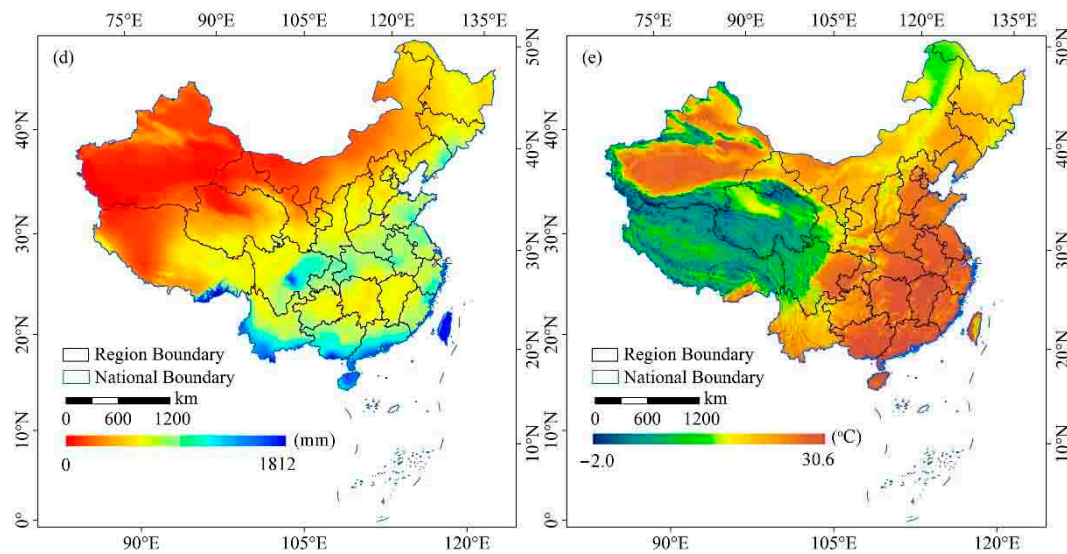
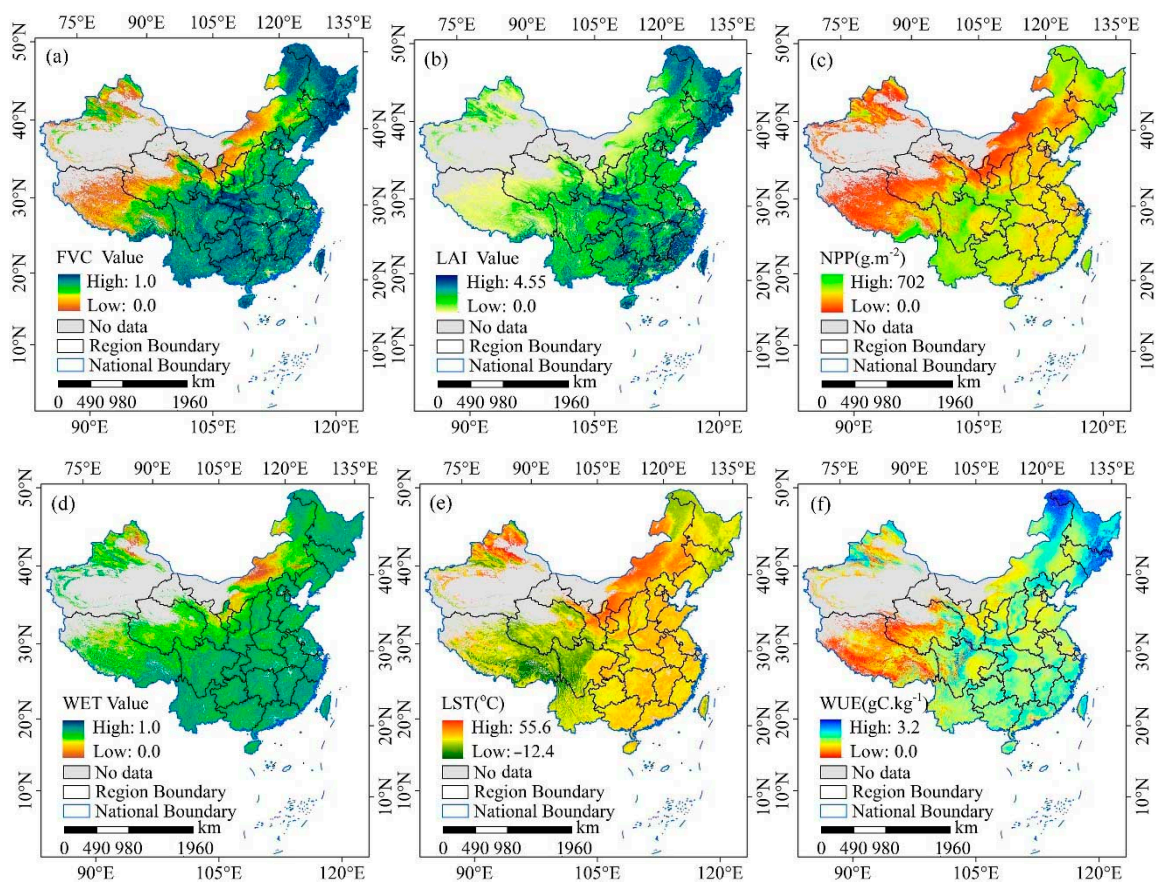


Figure 1. Cont.



**Figure 1.** (a) Spatial distribution of topographic and geographic zones, (b) the vegetation distribution, (c) the climate zones, (d) mean precipitation, and (e) mean temperature between 2000 and 2017 in the peak growing season of vegetation across China.



**Figure 2.** Spatial distribution of the average values of six indicators for vegetation ecology quality (VEQ) between 2000 and 2017 in the peak growing season of vegetation across China ((a–f) stand for fractional vegetation cover (FVC), leaf area index (LAI), net primary productivity (NPP), wetness (WET), land surface temperature (LST), and water use efficiency (WUE), respectively).

(2) Thickness indicator (*LAI*) (Figure 2b): *LAI* can further reflect the structure and biological characteristics of vegetation growth and represent the thickness exponent of vegetation. Extracting *LAI* from MODIS data has been validated in numerous scholarly studies [24–27]. The MOD15A2H was used to obtain *LAI* data for China in this study.

(3) Productivity indicator (*NPP*) (Figure 2c): *NPP* can reflect the photosynthetic intensity of plants and represents the indicator of vegetation productivity. The *NPP* data used in this study has been previously used to monitor the variation of forest cover and its impact on forest productivity in China. The data accuracy is reliable and can be utilized directly.

(4) Moisture indicator (*WET*) (Figure 2d): *WET* can be utilized to invert the integrated moisture of soil and vegetation and represent the moisture indicator of vegetation [28–30]. The MOD09A1 was utilized to calculate the moisture indicator of terrestrial vegetation in China based on the improved MODIS tassell cap transformation [31]. The formula is as follows:

$$WET = 0.1147\rho_1 + 0.2489\rho_2 + 0.2408\rho_3 + 0.3132\rho_4 - 0.3122\rho_5 - 0.6416\rho_6 - 0.5087\rho_7 \quad (5)$$

where  $\rho_i$  ( $i = 1, 2, \dots, 7$ ) is the reflectance of each band of MOD09A1.

(5) Heat indicator (*LST*) (Figure 2e): *LST* is a fine representation of vegetation variation and an important factor driving ecological change [32–34]. It is utilized to represent the heat indicator of vegetation. The surface temperature was calculated by MOD11A2.

(6) Suitability indicator (*WUE*) (Figure 2f): *WUE* refers to the water loss ratio of carbon absorption in each unit of vegetation ecosystem, which can represent the coupling extent of carbon and water [15]. It is also used to represent the suitability indicator of vegetation growth. The ratio of GPP to evapotranspiration was utilized to calculate *WUE*. GPP was acquired from MOD17A2H and evapotranspiration was acquired from GLASS ET.

### 2.3.2. Construction of VEQI

The proposed VEQI should integrate the characteristics of the above six indicators. Principal component analysis (PCA) can reduce data redundancy and reflect the information of the original variables as much as possible. It is also objective and can avoid human error [25]. It has already been used for spatial index calculations in the research of many scholars. Similarly, Liu et al. constructed the Remote-Sensing Ecological Index based on PCA to measure the ecological status of Bayinbruck [35]. Xu et al. constructed the Remote-Sensing Ecological Index based on PCA to quantify the ecological status of Fujian Province [30]. Yue et al. used PCA to research the ecological quality of 35 major cities in China [36]. Consequently, PCA was utilized to perform the analysis of dimensions reduced on six indicators. Firstly, the original data were standardized to eliminate the effects of disparate scales and dimensions [37], and the sample correlation coefficient matrix was calculated. Subsequently, the eigenvalues and eigenvectors of the sample correlation coefficient matrix were acquired and important principal components were also selected. Finally, the VEQI was obtained by the weighted summation formula. The standardized and weighted summation formulas are shown below, respectively [37].

$$X_i = [x_i - \min(x_i)] / [\max(x_i) - \min(x_i)] \quad (6)$$

$$VEQI = \sum_{i=1}^n k_i \lambda_i \quad (7)$$

where  $X_i$  is the standardized value of an indicator and  $x_i$  is the value of the indicator in pixel  $I$ ;  $k_i$  denotes the corresponding principal component  $I$ ;  $\lambda_i$  ( $i = 1, 2, \dots, n$ ) means the variance contribution ratio of the corresponding principal component, and  $n$  is the number of selected principal components. The results of PCA for four years, 2000, 2006, 2012, and 2017 at equal time intervals are presented for the exhibition (Table 1). The results of the remaining fourteen years are not listed in this paper due to space limitations. According to Table 1, the cumulative contributions of the first principal component (PC1) and the second principal component (PC2) to the VEQI in the four-period data are over 87%, indicating that

two principal components integrated most of the characteristics of all variables. Therefore, PC1 and PC2 were chosen to construct the VEQI.

**Table 1.** Result of principle component analysis (PCA) for six factors.

Indicator Factors	2000		2006		2012		2017	
	PC1	PC2	PC1	PC2	PC1	PC2	PC1	PC2
LST	−0.278	0.786	−0.281	0.861	−0.253	0.843	−0.237	0.911
WUE	0.043	0.724	0.083	0.831	0.191	0.853	0.155	0.751
NPP	0.921	0.283	0.92732	0.237	0.920	0.206	0.937	0.118
FVC	0.919	0.251	0.917	0.246	0.939	0.223	0.953	0.096
LAI	0.828	0.435	0.825	0.348	0.903	0.274	0.922	0.205
WET	0.451	0.753	0.431	0.736	0.455	0.799	0.399	0.886
Eigenvalue	3.113	1.878	3.086	2.336	3.158	2.245	2.967	2.250
Variance contribution/%	53.059	34.518	52.8255597	35.400	52.488	36.11	49.995	37.030
Cumulative contribution/%	53.059	87.577	52.827	88.227	52.488	88.590	49.995	87.025

To facilitate the measurement and comparison of indicators, the VEQI could also be standardized by the following formula:

$$VEQI_N = [VEQI_i - \min(VEQI_i)] / [\max(VEQI_i) - \min(VEQI_i)] \quad (8)$$

where  $VEQI_N$  is the standardized pixel value of  $VEQI_i$ , and  $VEQI_i$  is the unnormalized VEQI pixel value calculated by Equation (10). The  $VEQI_N$  values range between 0 and 1 with 1 denoting perfect VEQ status and 0 indicating an extremely poor one. The classification map of VEQ was also mapped using the ArcGIS 10.4 software.  $VEQI_N$  values were classified into five categories with an interval of 0.2, including poor (0–0.2), inferior (0.2–0.4), medium (0.4–0.6), good (0.6–0.8), and excellent (0.8–1).

### 2.3.3. Exploratory Spatial Data Analysis SEN + Mann–Kendall

The variation tendency of VEQ in China over the past 20 years was investigated using the Sen's slope and Mann–Kendall test. Compared with the commonly used trend analysis of the least square method, Sen's slope can effectively avoid the interference of abnormal values and measurement error [38]. Sen's slope was calculated as follows [38]:

$$Slope = \text{Median} \frac{VEQI_j - VEQI_i}{j - i} \quad 1 < i < j < n \quad (9)$$

where  $i$  and  $j$  are time ordinals; and  $VEQI_i$  and  $VEQI_j$  represent the pixel values of VEQI at  $i$  and  $j$  time, respectively.  $Slope > 0$  indicates an upward trend and  $Slope < 0$  illustrates a downward trend. The Mann–Kendall method was utilized to test the trend significance of the VEQI sequence. The calculation formulas are as follows:

$$U_{MK} = \begin{cases} (\tau - 1) / [Var(\tau)]^{\frac{1}{2}} & \tau > 0 \\ 0 & \tau = 0 \\ (\tau + 1) / [Var(\tau)]^{\frac{1}{2}} & \tau < 0 \end{cases} \quad (10)$$

$$\tau = \sum_{i=1}^{n-1} \sum_{j=i+1}^n \text{sign}(VEQI_j - VEQI_i) \quad (11)$$

$$\text{Sign}(VEQI_j - VEQI_i) = \begin{cases} 1 & VEQI_j - VEQI_i > 0 \\ 0 & VEQI_j - VEQI_i = 0 \\ -1 & VEQI_j - VEQI_i < 0 \end{cases} \quad (12)$$

$$Var(\tau) = \frac{n(n-1)(2n+5)}{18} \quad (13)$$

where  $U_{MK}$  is the test statistic;  $Var$  is the computed variance function;  $VEQI_j$  and  $VEQI_i$  are the VEQI values for year  $j$  and year  $i$ , respectively;  $Sign$  is the symbolic function, and  $n$  is the temporal sequence length. At a given level of significance  $p$ , when  $|U_{MK}| > \mu_{1-p/2}$  indicates that there is a significant change in the study sequence.

### Hurst Exponent

The Hurst exponent was utilized to describe the sustainability of the time-series VEQI. The basic principle is that for a given temporal variable  $\{\xi(t)\}$ , several sequences are constructed [39,40].

$$\text{Mean series : } \langle \xi \rangle_{\tau} = \frac{1}{\tau} \sum_{i=1}^{\tau} \xi(t) \quad \tau = 1, 2, \dots \quad (14)$$

$$\text{Cumulative discrepancy : } X(t, \tau) = \sum_{u=1}^{\tau} (\xi(u) - \langle \xi \rangle_{\tau}) \quad 1 \leq t \leq \tau \quad (15)$$

$$\text{Atrocious : } R(\tau) = X(t, \tau)_{\max} - X(t, \tau)_{\min} \quad \tau = 1, 2, \dots \quad (16)$$

$$\text{Standard deviation : } S(\tau) = \left[ \frac{1}{\tau} \sum_{i=1}^{\tau} (\xi(t) - \langle \xi \rangle_{\tau})^2 \right]^{\frac{1}{2}} \quad \tau = 1, 2, \dots \quad (17)$$

After calculating  $R(\tau)$  and  $S(\tau)$ ,  $R/S = R(\tau)/S(\tau)$  is defined. If  $R/S \propto \tau^H$ , it means that VEQI has the Hurst phenomenon in the time series, and  $H$  is the Hurst exponent. When  $H = 0.5$ , the series are random without temporal correlation. When  $0 < H < 0.5$ , it indicates that the future trend is opposite to the past, and the process has anti-sustainability. When  $0.5 < H < 1$ , it indicates that the future trend is consistent with the past, and the process has continuity. The greater  $H$  is, the more sustainable it is.

## 3. Results

### 3.1. Spatiotemporal Pattern of VEQ

#### 3.1.1. Spatial Distribution of VEQ

The distribution of VEQI in China had a strong spatial heterogeneity. Values of VEQI were low in the northwest and high in the northeast and southeast (Figure 3). Regions with poor and inferior VEQ were mainly distributed in arid and semi-arid areas (e.g., the Qinghai-Tibet Plateau, Inner Mongolia Plateau, Dzungarian Basin, and Tarim Basin) (Figure 3). Regions with good and excellent VEQ were predominately located in humid areas (e.g., the eastern and northern parts of northeast China, Qinling Mountains, Taiwan, Yangtze River basin, and southern China) (Figure 3). Regions of medium VEQ were concentrated in agricultural areas of dryland (e.g., the humid and semi-humid Sichuan Basin and North China Plain) (Figure 3). The average value of VEQI in the latitudinal direction was generally high, more than 0.7. The VEQ showed a decreasing trend with the latitude increasing, reaching the highest level at 42.5° N (Figure 4). The average value of VEQI was generally higher than 0.6 in the longitude direction. The VEQ represented an ameliorative trend with longitude increasing, reaching the highest level at 120.9° E (Figure 4).

For the pixel statistics, the mean of VEQI grids over the past 18 years was 0.540 with a standard deviation of 0.182. The poor and inferior VEQ regions accounted for 23.98% of the total vegetation zone, much lower than that of the good and excellent VEQ regions (40.74%). The medium VEQ regions accounted for 35.28% of the vegetation zone. This spatial distribution indicated that a difference existed between the high and low VEQ regions, with the high VEQ regions accounting for a much larger proportion than the low VEQ regions.

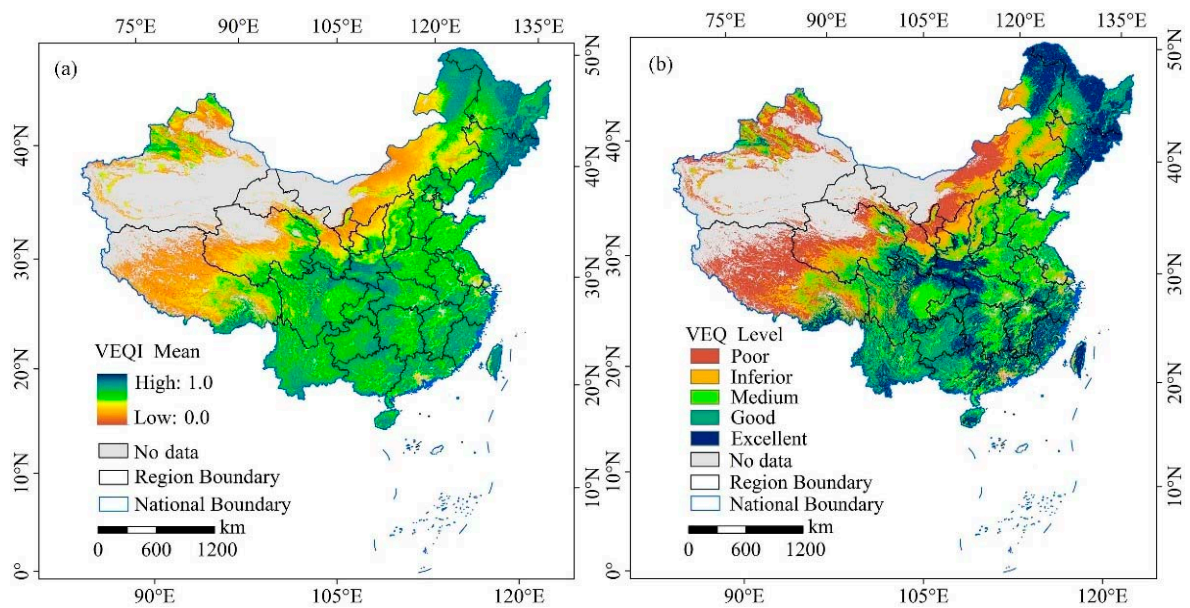


**Figure 3.** Spatial distribution of the average value (a) and level (b) of vegetation ecology quality index (VEQI) in China from 2000 to 2017.

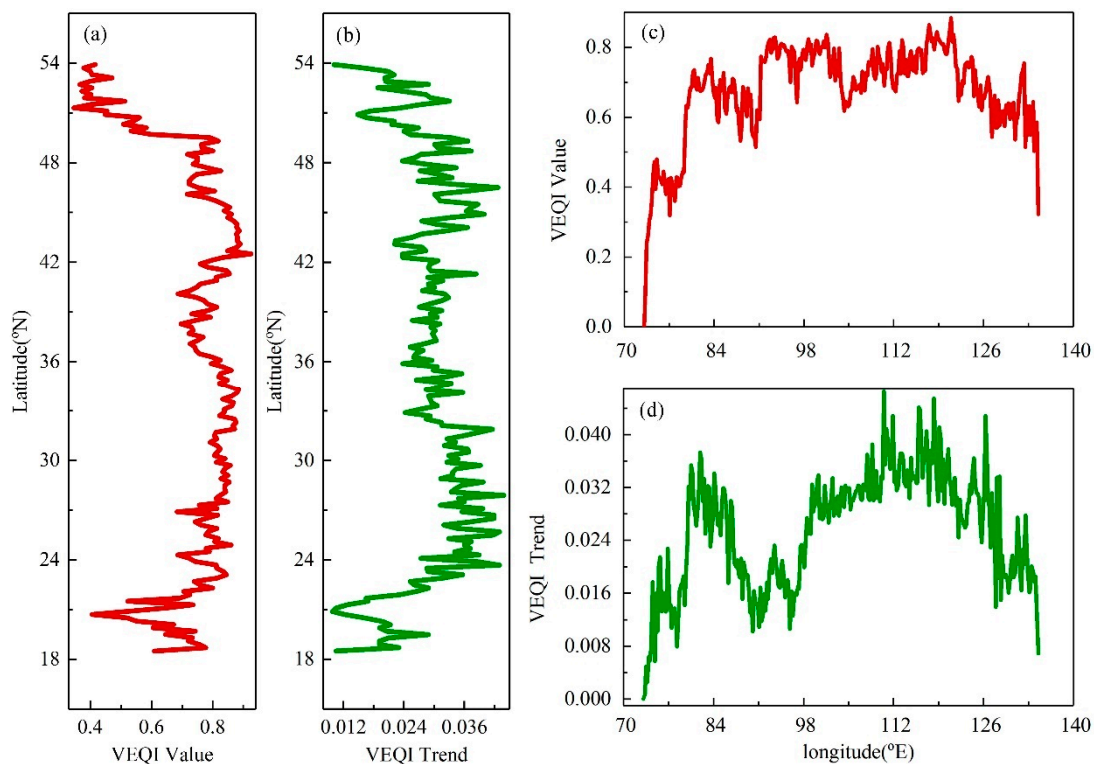


**Figure 4.** Distribution and variation trend of VEQI along latitude and longitude in China from 2000 to 2017 ((a,b) represent the distribution and variation trend of VEQI in latitude, (c,d) represent the distribution and variation trend of VEQI in longitude, respectively).

### 3.1.2. The Change Trend and Amplitude of VEQ

The tendency analysis manifested that the trend coefficient of VEQI in China was 0.0014, with a standard deviation of 0.002. The regions with increasing, almost constant, and decreasing VEQI accounted for 35.27%, 53.85%, and 10.88% of the total vegetation area, respectively (Figure 5). The trend coefficient was greater than 0 and the area of the region

with increasing VEQI was much larger than that of the region with decreasing VEQI, which indicated that the VEQ in China showed an ameliorative trend over the past 18 years.

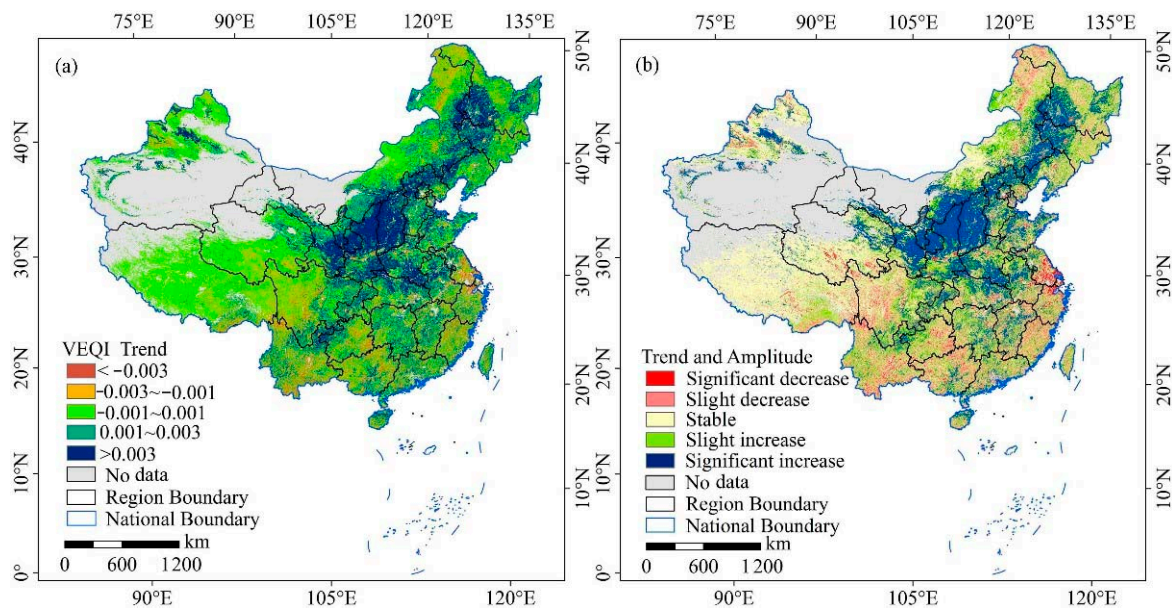


**Figure 5.** Spatial distribution of the variation trend of VEQ in China from 2000 to 2017.

The VEQI area of significant increase ( $p < 0.05$  and  $slope > 0.003$ ) accounted for 20.2% of the total vegetation area (Figure 5), with latitudes ranging from 23° E to 46.5° E and longitudes ranging from 101° E to 127° E (Figure 4), and chiefly distributed in sub-humid and semi-arid zones (e.g., the Loess Plateau (the most severely eroded region in the world), Qinling Mountains, Qilian Mountains, Northeast Plain, and parts of the Tianshan Mountains) (Figure 5). The VEQ area with a significant decrease ( $p < 0.05$  and  $slope < -0.003$ ) accounted for 2.76% (Figure 5), ranging from 27° E–34° E in latitude and 118° E–122° E in longitude (Figure 4), predominately located in the Lower Yangtze plains (Figure 5) that had seriously been affected by human disturbance. The regions with slight increase ( $p > 0.05$  and  $0.001 < slope < 0.003$ ) and slight decrease ( $p > 0.05$  and  $-0.003 < slope < -0.001$ ) were mainly situated in the monsoon climate zone (e.g., the vast regions of northeastern and southern China), accounting for 15.07% and 8.12%, respectively (Figure 5). Regions remained stable ( $-0.001 < slope < 0.001$ ) accounted for 53.85%, and were chiefly situated in the high-altitude and low-temperature regions (e.g., the Qinghai-Tibet Plateau, Tianshan Mountains and Altai Mountains) (Figure 5).

### 3.1.3. The Sustainability and Direction of VEQ in the Future

In terms of sustainability, the average Hurst exponent of VEQ in China was 0.569 over the past 18 years by a pixel-by-pixel calculation (Figure 6a). It was greater than 0.5 and indicated that the VEQ tendency of China in the future will be consistent with the past 18 years. That is, it will be sustainable. The area with Hurst exponent greater than 0.5 accounted for 78.92% of the total vegetation area and it exhibited a staggered distribution across most of China (Figure 6a and Table 2). The Hurst exponent of VEQ less than 0.5 suggested that the future change direction of the VEQ will be opposite to the past, namely, not sustainable, which only accounted for 21.08% and chiefly distributed in the northern part of the North China Plain, the northern Tianshan Mountains, and the southwestern part of the Northeast Plain (Figure 6a and Table 2). The VEQ protection efforts need to be further strengthened, especially in regions with unsustainable characteristics.

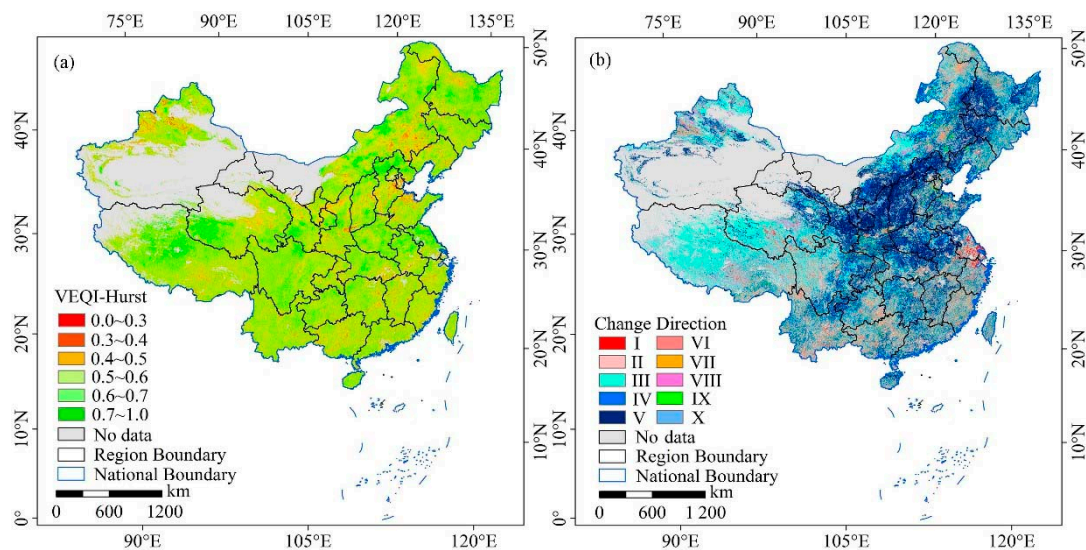


**Figure 6.** Spatial distribution of VEQI-Hurst exponent (a) and the spatial variation characteristics of the coupling of VEQI trend and Hurst exponent (b) in China from 2000 to 2017 (I-X mean sustained significant decrease, sustained not-significant decrease, basic stability, sustained not-significant increase, sustained significant increase, not-sustained significant decrease, not-sustained not-significant decrease, not-basic stability, not-sustained not-significant increase, and not-sustained significant increase, respectively).

**Table 2.** The predicted VEQ in China.

Hurst Exponent	Trend Coefficient ( <i>Slope</i> ) and Significance ( <i>P</i> )	VEQ forecast type	Area Percentage (%)
$0.5 < H < 1$	$Slope < -0.003; P < 0.05$	Sustained significant decrease	1.69
$0.5 < H < 1$	$-0.003 < Slope < -0.001; P > 0.05$	Sustained not-significant decrease	5.87
$0.5 < H < 1$	$-0.001 < Slope < 0.001; P > 0.05$	Basic stability	41.13
$0.5 < H < 1$	$0.001 < Slope < 0.003; P > 0.05$	Sustained not-significant increase	15.14
$0.5 < H < 1$	$Slope > 0.003; P > 0.05$	Sustained significant increase	15.09
$0 < H < 0.5$	$Slope < -0.003; P < 0.05$	Not-Sustained significant decrease	1.23
$0 < H < 0.5$	$-0.003 < Slope < -0.001; P > 0.05$	Not-Sustained not-significant decrease	1.72
$0 < H < 0.5$	$-0.001 < Slope < 0.001; P > 0.05$	Not-Basic stability	9.53
$0 < H < 0.5$	$0.001 < Slope < 0.003; P > 0.05$	Not-Sustained not-significant increase	4.23
$0 < H < 0.5$	$Slope > 0.003; P > 0.05$	Not-Sustained significant increase	4.37

To reveal the change direction of VEQ in the future, by superimposing the spatial pattern of Hurst exponent and the variation trend map of VEQ, comprehensive information of the trend and sustainability of VEQ in the future was obtained. The results were summarized into ten categories, as shown in Figure 6b and Table 2. For regions with VEQI-Hurst exponent greater than 0.5, the area of sustained significant decrease and sustained not-significant decrease accounted for 7.56% of the total vegetation area, predominately distributed in the lower reaches of the Yangtze River and Yun-Gui Plateau. The area of basic stability accounted for 41.13%, mainly situated in the Qinghai-Tibet Plateau, Tianshan Mountains, Altai Mountains, and the eastern Inner Mongolian Plateau. The area of sustained not-significant increase and sustained significant increase accounted for 30.23%, chiefly located in the Qilian Mountains, Loess Plateau, Northeast Plain, North China Plain, Qinling Mountains, Sichuan Basin, and the parts of Tianshan Mountains. For region with VEQI-Hurst exponent less than 0.5, the area of not-sustained significant decrease and not-sustained not-significant decrease accounted for 2.95% of the total vegetation area, which were predominately distributed in the south of Yangtze River basin and local area of the Great Hinggan Mountains. The area of not-basic stability accounted for 9.53%, mainly situated in the Qinghai-Tibet Plateau, Tianshan Mountains, Altai Mountains, and

the eastern Inner Mongolia Plateau. The area of not-sustained not-significant increase and not-sustained significant increase accounted for 8.6%, chiefly located in the Loess Plateau, Northeast Plain, and the northern Tianshan Mountains. The future construction of VEQ needs a precise strategy to strengthen the protection of VEQ in fluctuating and degraded areas.

### 3.2. The Characteristics of VEQ in Different Ecosystems

This study further analyzed the mean, trend, persistence and correlation of VEQI with altitude under different ecosystems (Table 3). The VEQI of broadleaved forest was the highest (Table 3), which was chiefly distributed in the warm and humid monsoon climate zones. Shrubs and arctic grass were predominantly located in the dry and cold climate zones, with low average VEQI values of 0.327 and 0.296, respectively (Table 3), which were substantially lower than those of other ecosystems. Average VEQI values ranged from 0.494 to 0.685 for coniferous forest, grassland, permanent wetlands, paddy field-dominated vegetation, dry cropland-dominated vegetation, and mixed cropland (Table 3). The VEQ in all ecosystems exhibited an ameliorative tendency over the past 18 years, with the three most significant improvements being in mixed cropland, dry cropland-dominated vegetation, and grassland (Table 3). The Hurst exponent of VEQI ranged from 0.56 to 0.60 for all ecosystems (Table 3), indicating that the future trend of VEQ in all ecosystems was consistent with that in the past 18 years and would be improved continually. Except for desert vegetation and paddy field-dominated vegetation, the average VEQI values were significantly negatively correlated with altitude. The higher correlation coefficients were shrubs and arctic grass, with R values of  $-0.405$  and  $-0.517$ , respectively (Table 3).

**Table 3.** The mean, trend, persistence, and correlation of VEQ with altitude in different ecosystems.

Ecosystem Type	Grid Counts	VEQI Value			Altitude		
		Mean Value	Trend (Per Year)	Hurst Exponent	Mean Value (m)	R	
Forest vegetation	Coniferous forest	635,367	0.685	0.00106	0.5672	1189	$-0.308$
	Broadleaved forest	659,414	0.731	0.00131	0.5692	857	$-0.113$
	Shrubs	558,158	0.643	0.00149	0.5690	1398	$-0.405$
Low-height natural vegetation	Arctic grass	920,397	0.327	0.00010	0.5908	4600	$-0.517$
	Grassland	1,700,267	0.494	0.00209	0.5648	1692	$-0.171$
	Permanent wetlands	90,494	0.588	0.00155	0.5684	1161	$-0.355$
	Desert vegetation	408,587	0.296	0.00148	0.5642	2970	0.061
Artificially cultivated vegetation	Paddy field-dominated vegetation	444,124	0.625	0.00159	0.5679	274	0.189
	Dry cropland-dominated vegetation	1,278,668	0.580	0.00269	0.5658	603	$-0.302$
	Mixed cropland	166,657	0.598	0.00359	0.5640	681	$-0.148$

#### 3.2.1. The Distribution and Trend of VEQ for Ecosystems within Climatic Zones

Further comparisons were made for the average VEQI of each ecosystem within the disparate climate zones (Figure 7a). The average VEQI in the tropical monsoon climate zone was the highest and that in the plateau mountain climate zone was the lowest. The difference of VEQI between forest vegetation and artificially cultivated vegetation were small in disparate climate zones. The VEQI of low-height natural vegetation differed considerably across disparate climate zones, with arctic grass showing the greatest difference in the tropical monsoon climate zone and temperate monsoon climate zone. VEQI was the highest for forest vegetation and the lowest for artificially cultivated vegetation in the tropical monsoon climate zone, with a discrepancy of 0.114. Except for arctic grass and desert vegetation, the average VEQI value of vegetation ecosystems demonstrated moderate in the subtropical monsoon climate zone and temperate monsoon climate zone. In the temperate monsoon climate zone, except shrubs, the average VEQI value of low-height natural vegetation was low, ranging from 0.218 to 0.37. In the plateau mountain climate zone, except for coniferous forest, broadleaved forest, and paddy field-dominated vegetation where the average VEQI was greater than 0.61, the average VEQI value of vegetation ecosystems was smaller, generally below 0.51.

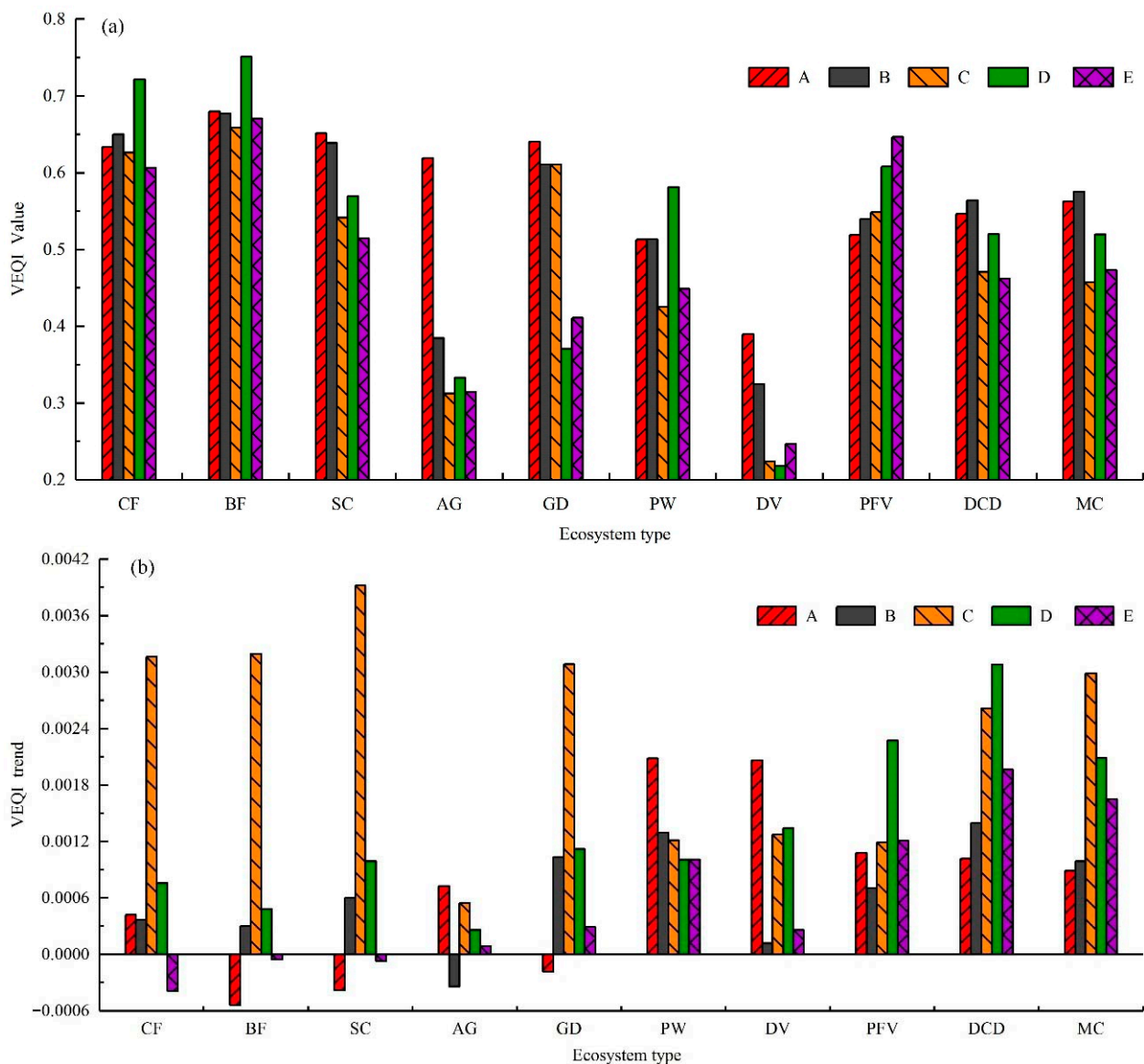


**Figure 7.** The average values (a) and change trends (b) of VEQI in disparate ecosystems and climate zones (Note: The alphabets A–E mean the climate zone column indicate the tropical monsoon climate zone, the subtropical monsoon climate zone, the temperate monsoon climate zone, the temperate continental climate zone, and the plateau mountain climate zone, respectively. CF is coniferous forest. BF is broadleaved forest. SC is shrubs. AG is arctic grass. GD is grassland. PW is permanent wetlands. DV is desert vegetation. PFV is paddy field-dominated vegetation. DCD is dry cropland-dominated vegetation. MC is mixed cropland).

In terms of the variation tendency of VEQ in ecosystems within different climatic zones, the VEQ of five climate zones exhibited an improvement, especially in the temperate monsoon climate zone (Figure 7b). The VEQ of broadleaved forest, shrubs, and grassland manifested a decreasing trend, while the VEQ of other ecosystems presented an ameliorative trend. The tropical monsoon climate zone showed an upward trend in VEQ of all vegetation types except for broadleaved forest, shrubs, and grassland, which presented a downward tendency. The VEQ in the subtropical monsoon climate zone showed an ameliorative trend in all vegetation types except for arctic grassland, which demonstrated a declining trend. The VEQ of all vegetation types displayed an ameliorative trend in the temperate monsoon and temperate continental climate zones. In the plateau mountain climate zone, the VEQ of coniferous forest, broadleaved forest, and shrubs pre-

sented a faint downward trend, while the VEQ of other vegetation types demonstrated an ameliorative trend.

### 3.2.2. The Distribution and Trend of VEQ for Ecosystems within Different Altitudes

As shown in Figure 8a, the average values of VEQI were further analyzed for each ecosystem at disparate altitude ranges. The average value of VEQI for forest vegetation decreased overall with increasing altitude, with smaller difference below 4 km. Except for shrubs, the average value of VEQI for the low-height natural vegetation did not vary significantly with the altitude below 4 km. When the altitude was greater than 4 km, the average value of VEQI decreased with the increase in altitude. The average value of VEQI for artificially cultivated vegetation did not vary significantly with the altitude below 2.8 km, and decreased with increasing altitude at the altitude greater than 2.8 km. The average VEQI reached the maximum value of 0.55 in the region with the altitude less than 570 m and the minimum value of 0.26 in the region with the altitude greater than 5200 m.

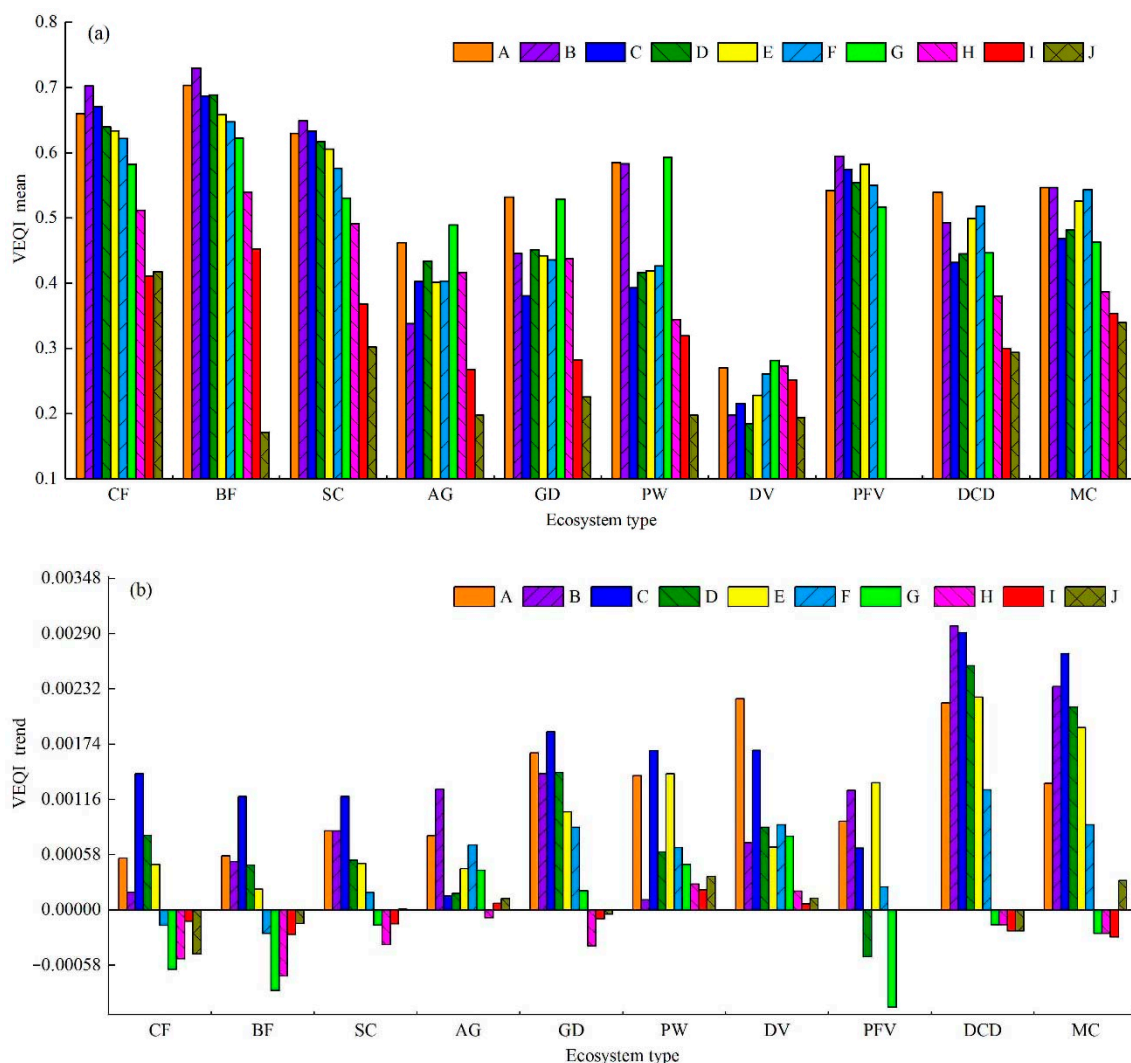


**Figure 8.** The average values (a) and variation trends (b) of VEQI in disparate ecosystems and disparate altitude zones (Note: A: 0–572 m, B: 572–1144 m, C: 1144–1716 m, D: 1716–2288 m, E: 2288–2860 m, F: 2860–3432 m, G: 3432–4004 m, H: 4004–4576 m, I: 4576–5148 m, J: 5148–8668 m. CF is coniferous forest. BF is broadleaved forest. SC is shrubs. AG is arctic grass. GD is grassland. PW is permanent wetlands. DV is desert vegetation. PFV is paddy field-dominated vegetation. DCD is dry cropland-dominated vegetation. MC is mixed cropland).

This study further analyzed the VEQ trends of each ecosystem at different altitude ranges (Figure 8b). The VEQ of forest vegetation improved in the region with the altitude less than 2.8 km. Degradation occurred in the region with altitude greater than 2.8 km. Low-height natural vegetation, permanent wetland, and desert vegetation improved at all altitude levels and arctic grassland and grassland improved at the altitude below 4 km and degraded at the altitude above 4 km. Shrubs degraded in the altitude range of 3.4 km–5.1 km and improved at the other altitude. For artificially cultivated vegetation, the variation tendency of VEQ was irregular along with the altitude, except for dry cropland-dominated vegetation, where the variation trend of VEQ was more regular along with the altitude. As a whole, VEQ improved below 3.4 km and degraded above 3.4 km over the past 18 years. Simultaneously, VEQ improved most significantly within the altitude range of 1.1 km to 1.7 km, and deteriorated most significantly within the altitude range of 4 km to 4.5 km.

### 3.3. The Relationship between VEQ and Climate Factors

#### 3.3.1. Climate Change and its Correlation with VEQ in Space

Climate change affects vegetation ecology through changes in temperature and altered hydrology. Precipitation during the peak growing season of vegetation exhibited an increasing tendency in most parts of China over the past 18 years, with the area of increased precipitation accounting for 84.35% of the total vegetation area, mainly distributed in the Loess Plateau, northwestern Northeast Plain, Yangtze River basin, and most of its southern regions (Figure 9a). The regions where precipitation increased by more than 10 mm were predominately located in the Sichuan Basin and north of the North China Plain (Figure 9a). The regions with decreasing precipitation during the peak growing season of vegetation were chiefly located in the lower Yellow River basin, southeastern part of Qinghai-Tibet Plateau and parts of southeastern China (Figure 9a), and the area with reduced precipitation only accounted for 15.65% of the total vegetation area. The temperature during the peak growing season also exhibited an increasing tendency, with the increase in temperature accounting for 88.26% of the total vegetation area, mainly distributed in most regions except the Tarim Basin and Inner Mongolian Plateau (Figure 9b). The areas with a temperature rise of more than 0.06 °C were predominately located in southeast China (Figure 9b).

According to the statistics of grid pixels, about 71.96% of the VEQI grids were positively correlated with precipitation, and about 52.75% of the VEQI grids were negatively correlated with temperature, which showed that precipitation was the main factor influencing the spatial distribution of VEQ. The response of VEQ to temperature and precipitation varied from region to region. The positive correlation between VEQI and precipitation was distributed throughout China, especially in the Inner Mongolia Plateau, Loess Plateau, Northern Xinjiang, and North China Plain, where the correlation between VEQI grids and precipitation was significant (Figure 9c). The regions where the VEQI grid had a significant negative correlation with precipitation were mainly situated in the high-latitude Great Hinggan Mountains (Figure 9c). The regions where the VEQI grid was negatively correlated with temperature were chiefly located in the Inner Mongolia Plateau, North China Plain, and Middle-Lower Yangtze Plain, while the regions where it was positively correlated were predominately located in alpine regions (e.g., the Qilian Mountains, Qinghai-Tibet Plateau, Tianshan Mountains, and Great Hinggan Mountains) (Figure 9d). On the whole, the VEQ during the peak growing season in China was negatively correlated with temperature and positively correlated with precipitation, and the influence of precipitation on VEQ was stronger than that of temperature.

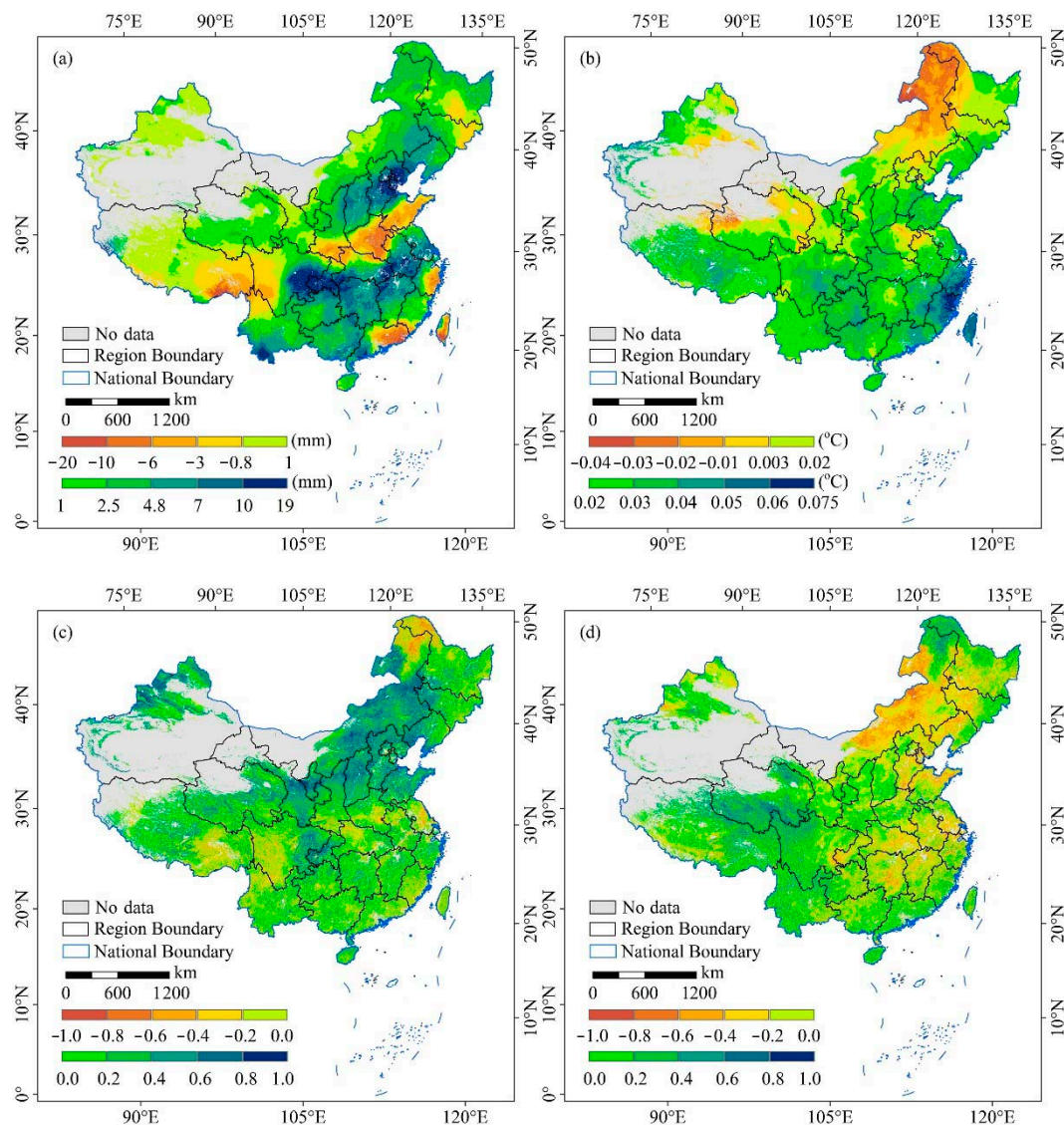


**Figure 9.** Spatial variation trends of the (a) precipitation and (b) temperature from 2000 to 2017, and the correlation coefficients between the VEQ and precipitation (c), temperature (d) during the peak growing season of vegetation.

### 3.3.2. The Correlation between VEQ and Climate Factors for Different Ecosystem

Temperature and precipitation have different effects on VEQ in different ecosystems. This study further analyzed the correlation coefficients of VEQ and temperature and precipitation under different ecosystems. According to the Table 4, VEQI and precipitation were positively correlated for all ecosystems. Larger correlation coefficients included ecosystems of grassland and dry cropland-dominated vegetation, which indicated that precipitation had a large effect on the VEQ of both ecosystems. Contrarily, smaller correlation coefficients included ecosystems of coniferous forest and broadleaved forest, with R-values of only 0.008 and 0.037, respectively, which indicated that precipitation has less impact on both ecosystems. VEQI was negatively correlated with temperature in ecosystems of grassland, paddy field-dominated vegetation, dry cropland-dominated vegetation, and mixed cropland, which suggests that high temperature was detrimental to growth of the four types of vegetation. The increased rate of warming accelerated the dissipation of soil moisture as well as vegetation moisture, which inhibited the activity of the four types of vegetation.

**Table 4.** The average values of precipitation and temperature in disparate ecosystems and analysis of their correlation with VEQ.

Ecosystem Type		Precipitation			Temperature		
		Mean Value (mm)	R	P	Mean Value (°C)	R	P
Forest vegetation	Coniferous forest	136	0.008	0.436	19.44	0.046	0.461
	Broadleaved forest	157	0.037	0.455	19.46	0.014	0.496
	Shrubs	149	0.083	0.450	19.77	0.022	0.488
Low-height natural vegetation	Arctic grass	74	0.162	0.416	5.79	0.240	0.349
	Grassland	89	0.289	0.261	16.45	−0.082	0.438
	Permanent wetlands	86	0.110	0.345	14.90	0.047	0.366
	Desert vegetation	63	0.213	0.320	11.45	0.077	0.437
Artificially cultivated vegetation	Paddy field-dominated vegetation	147	0.114	0.420	24.06	−0.150	0.424
	Dry cropland-dominated vegetation	117	0.285	0.281	21.05	−0.140	0.466
	Mixed cropland	129	0.228	0.332	21.42	−0.086	0.481

### 3.3.3. Impact of Climatic Factors on the VEQ of Different Ecosystems at Different Range

The impact of meteorological factors on the VEQ of different ecosystems at disparate range was further analyzed (Table 5). Precipitation and temperature during the peak growing season of vegetation had disparate impact on the VEQ at disparate range and ecosystem types. The ecosystems of coniferous forest and broadleaved forest were impacted by precipitation more regularly, with precipitation in the range of 18–108 mm promoting healthy vegetation growth. This impact was uncertain when precipitation exceeded 109 mm. The other eight ecosystems had irregular response to precipitation.

**Table 5.** The response of disparate ecosystems to precipitation and temperature in disparate ranges.

Vegetation	Precipitation Value Range (mm)				Temperature Value Range (°C)			
	Scope	Positive	Negative	Fluctuating	Scope	Positive	Negative	Fluctuating
Coniferous forest	18–594	18–108	—	108–594	3–27	3–12	12–23	23–27
Broadleaved forest	10–875	10–109	—	109–875	6–27	6–17	17–27	—
	Shrubs	11–419	11–168	—	168–419	1–27	1–23	23–27
Arctic grass	0–261	13–261	0–13	—	−1–26	−1–26	—	—
Grassland	0–187	0–100	—	100–187	2–26	2–13	13–26	—
Permanent wetlands	4–311	4–85	148–311	85–148	0–27	0–13	13–23	23–27
Desert vegetation	0–356	12–356	0–12	—	−2–27	−2–10	10–18	18–27
Paddy field-dominated vegetation	25–535	25–74	174–535	74–174	16–27	—	16–27	—
Dry cropland-dominated vegetation	3–244	3–38, 54–169	38–54	169–244	8–27	—	8–15	15–27
	Mixed cropland	5–589	5–172	—	172–589	8–27	8–17	17–24

Except for arctic grassland and desert vegetation ecosystems, the other ecosystems had temperature values between 0 °C and 27 °C during the peak growing season of vegetation. At relatively low temperatures, generally around 0 °C to 13 °C, there was a positive impact of temperature on the VEQ in most ecosystems. The impact of temperature on VEQ was negative or indeterminate when a vegetated ecosystem exceeded a certain temperature threshold.

## 4. Discussion

### 4.1. Spatial Distribution and Change Trend of the VEQ

The VEQ of China exhibited a deteriorating tendency with increasing latitude and an ameliorative trend with increasing longitude. This spatial distribution can be explained by the combination of various climatological variables [41,42], such as precipitation in China increasing significantly from west to east along longitude, the temperature descended from south to north along latitude, and VEQ degenerated with increasing altitude (Figure 1d,e). The poor and inferior VEQ may be limited by soil, topography, temperature, and precipitation. Simultaneously, for the main land covered by desert, gobi, and alpine vegetation, the proportion of vegetation area was small and the growth status of vegetation was terri-

ble. The excellent VEQ regions were mainly by temperate deciduous forest, laurilignosa, mixed coniferous broadleaved forest, and deciduous coniferous forest, as well as tropical rainforest, with suitable hydrothermal conditions and decent vegetation growth [2].

The VEQ in China displayed a continuously ameliorative trend from 2000 to 2017, which was indirectly consistent with the study by Liu et al. [2] on the change of vegetation in the growing season. The VEQ was impacted by both of climate and human activities. In addition, rapid urbanization of China in recent decades resulted in the shift of land-use patterns and then it caused a profound impact on the VEQ (e.g., increasing buildings and decreasing plowland) [7]. For instance, due to urban sprawl in southeast China, substantial impervious surface replaced the natural surface landscape dominated by vegetation. The VEQ has degraded over the past nearly 20 years. However, since the 21st century, China has extensively implemented ecological management projects (e.g., the Grain for Green Program, Afforestation and the Three-North Shelter Forest Program), which has improved the regional ecological environment and steadily increased ecological benefits [43]. Moreover, intensive agriculture in China has also contributed to the greening of the world [9]. The significant increase of vegetation cover and ecological quality in the Loess Plateau, Qinling Mountains, and Qilian Mountains may be largely impacted by anthropogenic activities such as ecological management projects [44]. However, in the context of strong human intervention and rapid climate change, it will remain crucial to quantitatively distinguish the positive and negative contributions of climate change and human activities to the VEQ at the national scale. Moreover, this study indicates that the VEQ in China would continue to improve in the future. The prediction from Zhou et al. [45] also indicated that vegetation growth in China would be better than that in the past under two representative concentration pathways (RCP4.5 and RCP8.5) scenarios from 12 coupled model inter-comparison project phase 5 (CMIP5) models.

#### 4.2. The VEQ Characteristics of Different Ecosystem

Broadleaved forests had the highest average VEQI value and shrubs and arctic grass had the lowest average VEQI value. Broadleaved forests are the topmost vegetation type with upward vegetation development and its more stable growth is a concrete expression of the ecological balance of the geographical landscape. Meanwhile, broadleaved forests are mostly located in the monsoon area with good hydrothermal conditions, with relatively high biological production, and extremely rich resources of animals, plants, and fungi. Thus, the VEQ of broadleaved forests is relatively fine. Grassland ecosystem in China are mostly located in alpine and dry areas (e.g., the Qinghai-Tibet Plateau, the Inner Mongolian Plateau, and the Tianshan Mountains), which have terrible hydrothermal conditions and are not conducive to the healthy growth of vegetation. Therefore, the VEQ of grassland is poor. During the past 18 years, the most significant improvements of VEQ have been in mixed cropland, dry cropland-dominated vegetation, and grassland. Although the area of crop cultivation in China has remained relatively stable since 2000 (about  $1.92 \times 10^6$  km<sup>2</sup>), the harvested area has generally shown an increasing trend year by year [9]. According to statistics from the Food and Agriculture Organization [46], total cereal production of China increased from  $407 \times 10^6$  tons in 2000 to  $583 \times 10^6$  tons in 2016, an increase of 43%. That was largely due to the increase in harvested area through multiple crops, which had led to the observed greening trend. Intensive agriculture in China has also been facilitated by the extensive use of chemical fertilizers and surface or groundwater irrigation [9]. These two factors have led to a significant improvement of VEQ in both mixed cropland and dry cropland-dominated vegetation. The improvement of VEQ in grassland may be mainly controlled by precipitation. Meanwhile, the improvement of human activities (e.g., overgrazing and the implementation of the return of cropland to grassland) have also played an important role in the increase for VEQ of grassland in recent years.

Overall, the average VEQI values of natural vegetation ecosystems were not significantly different below 4 km. When the altitude is greater than 4 km, the average value of VEQI decreases with the increase of altitude. This is because the zones with altitude greater

than 4 km in China are mainly located in the alpine regions such as the Qinghai-Tibet Plateau and the Tianshan Mountains. Seriously affected by the topographic height, the water and heat conditions in these areas are poor, which is not conducive to the healthy growth of vegetation. Furthermore, the higher the altitude, the worse the ecological quality of vegetation. The improvement of VEQ in low elevation areas throughout the study period may be mainly influenced by climate and human activities. The increase of precipitation in the low elevation area during the vegetation growth season in the last 18 years has promoted the healthy growth of vegetation. Human activities (e.g., afforestation, grazing ban, reforestation, etc.) have also greatly contributed to the improvement of VEQ.

#### 4.3. Impact of Meteorological Factors on the VEQ and Research Deficiencies

Precipitation during the peak growing season of vegetation has disparate impact on VEQ at different ranges. Precipitation can regulate the activities of vegetation within a certain range, which is conducive to the healthy growth of vegetation. Superabundant precipitation leads to fewer hours of sunshine, which is not conducive to the photosynthesis of plants. In addition, excessive precipitation can cause scour and erosion on the ground surface and destroy vegetation [47]. There is a positive effect of temperature on the VEQ in most ecosystems at relatively low temperatures during the peak growing season of vegetation, and a negative or uncertain effect when temperature reaches above a certain threshold. According to existing studies, the response of vegetation activities to temperature is more pronounced as temperature increases in China [8]. Before the vegetation obtained the optimum temperature for photosynthesis, the increase of temperature would promote photosynthesis. When the temperature was exceeded, on the one hand, it increased the respiration of vegetation and accelerated the consumption of nutrients. On the other hand, it caused the acceleration of water evapotranspiration and the decrease in the accumulation of dry matter [48]. Therefore, vegetation activities in response to climate change reflected non-linear processes and compound effects. It is also necessary to detect the spatial distribution and temporal dynamics of VEQ from the perspective of multifactorial comprehensive analysis.

There are several deficiencies in this study. Firstly, VEQI was constructed by six indicators obtained from remote sensing data for evaluating the VEQ in China. While VEQ is a comprehensive concept that characterizes structural and functional attributes (e.g., productivity and coverage of vegetation), using six indicators to evaluate the VEQ may not be comprehensive enough. Therefore, newly developed indicators should be integrated later to propel the deepening and expansion of the research field of the VEQ. Secondly, some pixels in the remote sensing data had no values or large error values due to the interference of clouds and shadows. Hence, the research on the valueless pixel-fitting algorithm will be implemented to improve data accuracy in the future. Thirdly, the seasonal and lagged effects of temperature and precipitation on the VEQ were not considered. However, there were differences in the seasonal and lagged response of VEQ to precipitation and temperature in China, which chiefly exhibited significant differences among disparate regions, terrains, and other factors [4,5]. The seasonality and lags of VEQ to climatic factors (e.g., temperature and precipitation) will be considered in the future. Fourthly, land use in China was changing rapidly, and the map of vegetation types used in this study was mainly derived from China's land cover map based on the fusion of multiple sources of data in 2000. The distribution of vegetation types was treated as an invariant during the study, which inevitably had some impacts on our results. However, the objective of this study was chiefly vegetation. According to land transfer statistics in China, the transfer between land use in vegetated ecological zones was not significant compared to built-up land expansions [49]. Thus, the spatial difference of vegetation types would not bring any significant deviation to our research. Despite the above deficiencies, our findings still have important guiding significance for the eco-environmental departments to formulate relevant policies and manage eco-environmental resources.

## 5. Conclusions

The distribution of VEQ in China had a strong spatial heterogeneity from 2000 to 2017. The poor and inferior VEQ areas in China were mainly located in arid and semi-arid regions with weak hydrothermal conditions. The medium VEQ areas were concentrated in agricultural regions of dryland with average hydrothermal conditions. The good and excellent VEQ areas were chiefly distributed in humid and sub-humid areas with fine hydrothermal conditions, and with the proportion being much larger than those of the poor and inferior VEQ areas. VEQ demonstrated a decreasing trend with increasing latitude and an improving trend with increasing longitude. The VEQ in China has continued to improve over the past 18 years, and it should also continue to improve in the future.

The distribution and variation tendency of VEQ varied among ecosystems during the peak growing season of vegetation. Broadleaved forest had the best VEQ. Shrubs and arctic grassland had worse VEQ than other ecosystems. The VEQ presented an ameliorative trend in all ecosystems, with the most significant improvement in mixed cropland, dry cropland-dominated vegetation and grassland. Moreover, the VEQ differed from disparate altitudes and climatic zones. Except for desert vegetation and paddy field-dominated vegetation, there was a significant negative correlation between VEQ and altitude. VEQ was the best in the tropical monsoon climate zone and the worst in the plateau mountain climate zone.

On the whole, the VEQ during the peak growing season in China was negatively correlated with temperature and positively correlated with precipitation, and the influence of precipitation on VEQ was stronger than that of temperature. Precipitation within a certain range could accelerate vegetation growth, while excessive precipitation could inhibit vegetation growth. There were positive effects of temperature on the VEQ in most ecosystems at relatively low temperatures, and negative or uncertain effects above a certain temperature threshold. Our research can provide detailed guidance on how China can better adapt to climate change in the face of global warming.

**Author Contributions:** Conceptualization, C.L. and X.L.; methodology, C.L. and D.L.; software, F.C. and Y.H.; formal analysis, B.Z.; investigation, Q.Q.; resources, C.L. and B.Z.; writing—original draft preparation, C.L.; writing—review and editing, C.L. and X.L.; project administration, X.L.; funding acquisition, X.L. All authors have read and agreed to the published version of the manuscript.

**Funding:** This work was financially supported by the National Natural Science Foundation of China (41761014), the Foundation of A Hundred Youth Talents Training Program of Lanzhou Jiaotong University and Excellent Platform of Lanzhou Jiaotong University.

**Institutional Review Board Statement:** Not applicable.

**Informed Consent Statement:** Not applicable.

**Data Availability Statement:** Not applicable.

**Acknowledgments:** Thanks to the National Tibetan Plateau Scientific Data Center and Cold and Arid Region Scientific Data Center for data support.

**Conflicts of Interest:** No potential conflict of interest was reported by the authors.

## References

- Ouyang, Z.Y.; Zheng, H.; Xiao, Y.; Polasky, S.; Liu, J.G.; Xu, W.H.; Wang, Q.; Zhang, L.; Xiao, Y.; Rao, E.M.; et al. Improvements in ecosystem services from investments in natural capital. *Science* **2016**, *352*, 1455–1459. [[CrossRef](#)]
- Liu, X.F.; Zhu, X.F.; Li, S.S.; Liu, Y.X.; Pan, Y.Z. Changes in growing season vegetation and their associated driving forces in China during 2001–2012. *Remote Sens.* **2015**, *7*, 15517–15535. [[CrossRef](#)]
- Wu, Y.J.; Zhao, X.S.; Xi, Y.; Liu, H.; Li, C. Comprehensive evaluation and spatial-temporal changes of eco-environmental quality based on MODIS in Tibet during 2006–2016. *Acta Geogr. Sin.* **2019**, *74*, 1438–1449. [[CrossRef](#)]
- Luo, H.X.; Wang, L.L.; Fang, J.H.; Li, Y.P.; Li, H.L.; Dai, S.P. NDVI, temperature and precipitation variables and their relationships in Hainan Island from 2001 to 2014 based on MODIS NDVI. In *Geo-Informatics in Resource Management and Sustainable Ecosystem, Proceedings of the International Conference on Geo-Informatics in Resource Management and Sustainable Ecosystem, Wuhan, China, 16–18 October 2015*; Springer: Berlin/Heidelberg, Germany, 2016; pp. 336–344.

5. Colditz, R.; Villanueva, V.L.A.; Tecuapetla-Gomez, I.; Gómez-Mendoza, L. Temporal relationships between daily precipitation and NDVI time series in Mexico. In Proceedings of the International Workshop on the Analysis of Multitemporal Remote Sensing Images (MultiTemp), Brugge, Belgium, 27–29 June 2017. [[CrossRef](#)]
6. Geng, L.Y.; Che, T.; Wang, X.F.; Wang, H.B. Detecting spatiotemporal changes in vegetation with the BFAST model in the Qilian Mountain region during 2000–2017. *Remote Sens.* **2019**, *11*, 103. [[CrossRef](#)]
7. Deng, X.Z.; Huang, J.K.; Rozelle, S.; Zhang, J.P.; Li, Z.H. Impact of urbanization on cultivated land changes in China. *Land Use Policy* **2015**, *45*, 1–7. [[CrossRef](#)]
8. Gao, J.B.; Jiao, K.W.; Wu, S.H. Investigating the spatially heterogeneous relationships between climate factors and NDVI in China during 1982 to 2013. *J. Geogr. Sci.* **2019**, *29*, 1597–1609. [[CrossRef](#)]
9. Chen, C.; Park, T.; Wang, X.H.; Piao, S.L.; Xu, B.D.; Chaturvedi, R.K.; Fuchs, R.; Brovkin, V.; Ciais, P.; Fensholt, R.; et al. China and India lead in greening of the world through land-use management. *Nat Sustain.* **2019**, *2*, 122–129. [[CrossRef](#)]
10. Liu, G.; Sun, R.; Xiao, Z.Q.; Cui, T.X. Analysis of spatial and temporal variation of net primary productivity and climate controls in China from 2001 to 2014. *Acta Ecol. Sin.* **2017**, *37*, 4936–4945. [[CrossRef](#)]
11. Long, S.; Guo, Z.F.; Xu, L.; Zhou, H.Z.; Fang, W.H.; Xu, Y.J. Spatiotemporal variations of fractional vegetation coverage in China based on Google Earth Engine. *Remote Sens. Technol. Appl.* **2020**, *35*, 326–334. [[CrossRef](#)]
12. Jiang, F.G.; Smith, A.R.; Kutia, M.; Wang, G.X.; Liu, H.; Sun, H. A modified KNN method for mapping the Leaf Area Index in arid and semi-arid areas of China. *Remote Sens.* **2020**, *12*, 1884. [[CrossRef](#)]
13. Chuai, X.W.; Guo, X.M.; Zhang, M.; Yuan, Y.; Li, J.S.; Zhao, R.Q.; Yang, W.J.; Li, J.B. Vegetation and climate zones based carbon use efficiency variation and the main determinants analysis in China. *Ecol. Indic.* **2020**, *111*, 105967. [[CrossRef](#)]
14. Zhang, Y.H.; Ye, A.Z. Spatial and temporal variations in vegetation coverage observed using AVHRR GIMMS and terra MODIS Data in the mainland of China. *Int. J. Remote Sens.* **2020**, *41*, 4238–4268. [[CrossRef](#)]
15. Shi, X.L.; Wu, M.Y.; Zhang, N. Characteristics of water use efficiency of typical terrestrial ecosystems in China and its response. *Trans. Chin. Soc. Agric. Eng.* **2020**, *36*, 152–159. [[CrossRef](#)]
16. Ran, Y.H.; Li, X. *Plant Functional Types Map in China*; Cold and Arid Regions Science Data Center: Lanzhou, China, 2011. [[CrossRef](#)]
17. Ran, Y.H.; Li, X.; Lu, L.; Li, Z.Y. Large-scale land cover mapping with the integration of multi-source information based on the dempster-shafer theory. *Int. J. Geogr. Inf. Sci.* **2012**, *26*, 169–191. [[CrossRef](#)]
18. Peng, S.Z.; Gang, C.; Cao, Y.; Chen, Y. Assessment of climate change trends over the Loess Plateau in China from 1901 to 2100. *Int. J. Climatol.* **2017**, *38*, 2250–2264. [[CrossRef](#)]
19. Peng, S.Z.; Ding, Y.X.; Wen, Z.M.; Chen, Y.M.; Cao, Y.; Ren, J.Y. Spatiotemporal change and trend analysis of potential evapotranspiration over the Loess Plateau of China during 2011–2100. *Agric. For. Meteorol.* **2017**, *233*, 183–194. [[CrossRef](#)]
20. Peng, S.Z.; Ding, Y.X.; Liu, W.Z.; Li, Z. 1 km monthly temperature and precipitation dataset for China from 1901 to 2017. *Earth Syst. Sci. Data* **2019**, *11*, 1931–1946. [[CrossRef](#)]
21. Peng, S.Z. *1-km Monthly Precipitation Dataset for China (1901–2017)*; National Tibetan Plateau Data Center: Beijing, China, 2020. [[CrossRef](#)]
22. Ding, Y.X.; Peng, S.Z. Spatiotemporal trends and attribution of drought across China from 1901–2100. *Sustainability* **2020**, *12*, 477. [[CrossRef](#)]
23. Ma, Z.C.; Yu, H.B.; Cao, C.M.; Zhang, Q.F.; Hou, L.L.; Liu, Y.X. Spatiotemporal characteristics of fractional vegetation coverage and its influencing factors in China. *Resour. Environ. Yangtze Basin* **2020**, *29*, 1310–1321. [[CrossRef](#)]
24. Ftnsholt, R.; Sandholt, I.; Rasmussen, M.S. Evaluation of MODIS LAI, FAPAR and the relation between FAPAR and NDVI in a semi-arid environment using in situ measurements. *Remote Sens. Environ.* **2004**, *91*, 490–507. [[CrossRef](#)]
25. Sabokbar, H.F.; Roodposhti, M.S.; Tazik, E. Landslide susceptibility mapping using geographically-weighted principal component analysis. *Geomorphology* **2014**, *226*, 15–24. [[CrossRef](#)]
26. Jensen, J.L.R.; Humes, K.S.; Hudak, A.T.; Vierling, L.A.; Delmelle, E. Evaluation of the MODIS LAI product using independent lidar-derived LAI: A case study in mixed conifer forest. *Remote Sens. Environ.* **2011**, *115*, 3625–3639. [[CrossRef](#)]
27. Liao, Y.R.; Gai, Y.Y.; Yao, Y.J.; Fan, W.J.; Xu, X.R.; Yan, B.Y. Validation methods of LAI products on the basis of scaling effect. *J. Remote Sens.* **2015**, *19*, 143–152. [[CrossRef](#)]
28. Kauth, R.J.; Thomas, G.S. The tasseled cap—A graphic description of the spectral-temporal development of agricultural crops as seen in Landsat. In Proceedings of the Symposium on Machine Processing of Remotely Sensed Data, West Lafayette, IN, USA, 29 June–1 July 1976; pp. 41–51.
29. Huang, C.Q.; Wylie, B.; Yang, L.; Homer, C.; Zylstra, G. Derivation of a tasseled cap transformation based on Landsat 7 at-satellit reflectance. *Int. J. Remote Sens.* **2002**, *23*, 1741–1748. [[CrossRef](#)]
30. Xu, H.Q.; Wang, Y.F.; Guan, H.D.; Shi, T.T.; Hu, X.S. Detecting ecological changes with a remote sensing based ecological index (RSEI) produced time series and change vector analysis. *Remote Sens.* **2019**, *11*, 2345. [[CrossRef](#)]
31. Lobser, S.E.; Cohen, W.B. MODIS tasseled cap: Land cover characteristics expressed through transformed MODIS data. *Int. J. Remote Sens.* **2007**, *28*, 5079–5101. [[CrossRef](#)]
32. Rhee, J.; Im, J.; Carbone, G.J. Monitoring agricultural drought for arid and humid regions using multi-sensor remote sensing data. *Remote Sens. Environ.* **2010**, *114*, 2875–2887. [[CrossRef](#)]
33. Weng, Q.; Fu, P.; Gao, F. Generating daily land surface temperature at Landsat resolution by fusing Landsat and MODIS data. *Remote Sens. Environ.* **2014**, *145*, 55–67. [[CrossRef](#)]

34. Xu, H.Q. Dynamic of soil exposure intensity and its effect on thermal environment change. *Int. J. Climatol.* **2014**, *34*, 902–910. [[CrossRef](#)]
35. Liu, Q.; Yang, Z.P.; Han, F.; Shi, H.; Wang, Z.; Chen, X.D. Ecological environment assessment in world natural heritage site based on Remote-Sensing Data. a case study from the Bayinbuluke. *Sustainability* **2019**, *11*, 6385. [[CrossRef](#)]
36. Yue, H.; Liu, Y.; Li, Y.; Lu, Y. Eco-environmental quality assessment in China's 35 major cities based on remote sensing ecological index. *IEEE Access.* **2019**, *7*, 51295–51311. [[CrossRef](#)]
37. Liu, D.; Hao, S. Ecosystem health assessment at county-scale using the pressure-state-response framework on the Loess Plateau, China. *Int. J. Environ. Res. Public Health* **2017**, *14*, 2. [[CrossRef](#)] [[PubMed](#)]
38. Liu, X.F.; Zhu, X.F.; Pan, Y.Z.; Li, S.S.; Zhang, D.H.; Liu, Y.X. The spatial-temporal changes of cold surge in Inner Mongolia during recent 53 Years. *Acta Geogr. Sin.* **2014**, *69*, 1013–1024. [[CrossRef](#)]
39. Wang, G.G.; Zhou, K.F.; Sun, L.; Qin, Y.F.; Li, X.M. Study on the vegetation dynamic change and R/S analysis in the past ten years in Xinjiang. *Remote Sens. Technol. Appl.* **2010**, *25*, 84–90. [[CrossRef](#)]
40. He, Y.; Yan, H.W.; Ma, L.; Zhang, L.F.; Qiu, L.S.; Yang, S.W. Spatiotemporal dynamics of the vegetation in Ningxia, China using MODIS imagery. *Front. Earth Sci.* **2020**, *14*, 221–235. [[CrossRef](#)]
41. Wang, S.X.; Yao, Y.Y.; Zhou, Y. Analysis of ecological quality of the environment and influencing factors in China during 2005–2010. *Int. J. Environ. Res. Public Health* **2014**, *11*, 1673–1693. [[CrossRef](#)]
42. Zhang, D.; Liu, X.M.; Zhang, L.; Zhang, Q.; Gan, R.; Li, X.H. Attribution of evapotranspiration changes in humid regions of China from 1982 to 2016. *J. Geophys. Res.-Atmos* **2020**, *125*. [[CrossRef](#)]
43. Gao, Y.; Zhu, X.J.; Yu, G.R.; He, N.P.; Wang, Q.F.; Tian, J. Water use efficiency threshold for terrestrial ecosystem carbon sequestration in China under afforestation. *Agric. For. Meteorol.* **2014**, *195*, 32–37. [[CrossRef](#)]
44. Zhao, T.; Bai, H.; Deng, C.H.; Meng, Q.; Guo, S.Z.; Qi, G.Z. Topographic differentiation effect on vegetation cover in the Qinling Mountains from 2000 to 2016. *Acta Ecol. Sin.* **2019**, *39*, 4499–4509. [[CrossRef](#)]
45. Zhou, Z.Q.; Ding, Y.B.; Shi, H.Y.; Cai, H.J.; Fu, Q.; Liu, S.N.; Li, T.X. Analysis and prediction of vegetation dynamic changes in China: Past, present and future. *Ecol. Indic.* **2020**, *117*, 106642. [[CrossRef](#)]
46. FAOSTAT, Food and Agriculture Organization (FAO). 2018. Available online: <http://www.fao.org/faostat/> (accessed on 1 August 2020).
47. Zhou, J.L.; Ma, M.G.; Xiao, Q.; Wen, J.G. Vegetation dynamics and its relationship with climatic factors in southwestern China. *Remote Sens. Technol. Appl.* **2017**, *32*, 966–972. [[CrossRef](#)]
48. Jiao, K.W.; Gao, J.B.; Wu, S.H.; Hou, W.J. Research progress on the response processes of vegetation activity to climate change. *Acta Ecol. Sin.* **2018**, *38*, 2229–2238. [[CrossRef](#)]
49. Zhang, M.; Huang, X.J.; Chuai, X.W.; Yang, H.; Lai, L.; Tan, J.Z. Impact of land use type conversion on carbon storage in terrestrial ecosystems of China: a spatial-temporal perspective. *Sci. Rep.* **2015**, *5*, 10233. [[CrossRef](#)] [[PubMed](#)]